Through-the-Mask (TTM) Optical Alignment for High Volume Manufacturing Nanoimprint Lithography Systems

Takamitsu Komaki, Yasuyuki Unno, Takahiro Matsumoto, Toshiki Iwai, Nozomu Hayashi, Tomokazu Taki, Tohru Kawashima, Satoshi Iino, Shinichirou Hirai, Ken Minoda, Takafumi Miyaharu, Kazuhiro Takahashi, Kazuhiko Mishima

Canon Inc., 20-2, Kiyohara-Kogyodanchi, Utsunomiya-shi, Tochigi 321-3292 Japan

Abstract

As the most aggressive features in advanced memory designs continue to shrink, so does the overlay budget. The number of layer stacks also creates unwanted topography, and the alignment robustness of lithography tools becomes much more important for on-product overly.

Canon developed a through-the-mask moiré alignment system for the FPA-1200NZ2C nanoimprint lithography (NIL) system allowing high-speed measurement of several alignment marks within each imprint field and alignment compensation to be completed during the imprinting sequence. To provide increased process flexibility and overlay accuracy while maintaining high-productivity, we have developed a new low-noise and high-resolution moiré diffraction alignment system based on spatial phase interferometry.

In this paper, we report on the TTM detection system used in FPA-1200NZ2C. In particular, the principle of moiré detection and the improvement of the detection method will be described. The measurement error of moiré is analyzed by a simplified model calculation and we confirmed the relationship between process change and alignment error. Results of analyses proved that selection of the wavelength are key factors for optimizing alignment accuracy. Based on these results we applied the following improvement items: 1) Dual Dipole illumination, 2) Optimization of the alignment wavelength.

We evaluated the new alignment system measurement error by comparing the moiré measurement value with the measured overlay values for 24 wafers and confirmed that new TTM alignment system can reduce to the measurement error more than 40%. The data shows that our moiré measurement system can provide process robustness and can support mass-production of leading-edge memory products.

Keywords: nanoimprint lithography, NIL, alignment, overlay, TTM, moiré, robustness, wavelength

1. Introduction

Imprint lithography is an effective and well known technique for replication of Nano-scale features.[1,2] Nanoimprint lithography (NIL) manufacturing equipment utilizes a patterning technology that involves the field-by-field deposition and exposure of a low viscosity resist deposited by jetting technology onto the substrate.[3-9] The patterned mask is lowered into the fluid which then quickly flows into the relief patterns in the mask by capillary action. Following this filling step, the resist is cross-linked under UV radiation, and then the mask is removed, leaving a patterned resist on the substrate. The technology faithfully reproduces patterns with a higher resolution and greater uniformity compared to those produced by photolithography equipment.

Canon is applying its NIL technology for advanced memory devices, such as 3D NAND Flash, DRAM and Phase Change Memory. Device scaling continues for both DRAM and Phase Change Memory. State of the art DRAM is now at 16nm. For 14nm, an overlay requirement of 15% - 20%, means meeting an overlay budget of 2.1 – 2.8nm. To meet this specification, along with enhancing productivity, NIL HVM readiness requires robust alignment and overlay solutions.

Optical Microlithography XXXIII, edited by Soichi Owa, Proc. of SPIE Vol. 11327, 113270Y
 · doi: 10.1117/12.2551980

Canon developed a through-the-mask moiré alignment system for the FPA-1200NZ2C nanoimprint lithography (NIL) system allowing high-speed measurement of several alignment marks within each imprint field and alignment compensation to be completed during the imprinting sequence. To provide increased process flexibility and overlay accuracy while maintaining high-productivity, we have developed a new low-noise and high-resolution moiré diffraction alignment system based on spatial phase interferometry.[10]

In this paper, we will report on the TTM detection system used in FPA-1200NZ2C. In particular, the principle of moiré detection and the improvement of the detection method will be described. The measurement error of moiré is analyzed by the simplified model calculation and confirmed relationship between process change and alignment error. Results of analyses proved that selection of the wavelength are key factors for optimizing alignment accuracy. Based on these test results we applied the following improvement items: 1) Dual dipole illumination, 2) Optimizing alignment wavelength.

We evaluated the new alignment system measurement error by comparing the moiré measurement value with the measured overlay values for 24 test wafers and confirmed that new TTM alignment system can reduce the measurement error by more than 40%. The data shows that our moiré measurement system can provide process robustness and can support mass-production of leading-edge memory products.

2. Thorough the Mask Alignment System

a. Through The Mask (TTM) Alignment System

The FPA-1200NZ2C system uses a Through the Mask (TTM) alignment system as shown in Figure 1. The mask and wafer are placed close to each other to observe the wafer mark through the mask. In order to perform die-by-die alignment, at least four alignment marks are arranged on the mask and the wafer. It is necessary to measure alignment at high speed to correct shot shift and shot low-order distortion from the start of imprinting to exposure.

The FPA-1200NZ2C consists of four main optical units. A spread camera is a unit for monitoring resist filling and monitoring imprint status. The High Order Distortion Correction (HDOC) unit performs high-order distortion correction by applying heat distribution to the wafer surface[11, 12]. The UV exposure unit cures the resist by exposure. A relay lens was developed to optically integrate these four units by splitting the wavelength with a dichroic mirror, allowing them to function simultaneously. The alignment is performed through the relay lens.

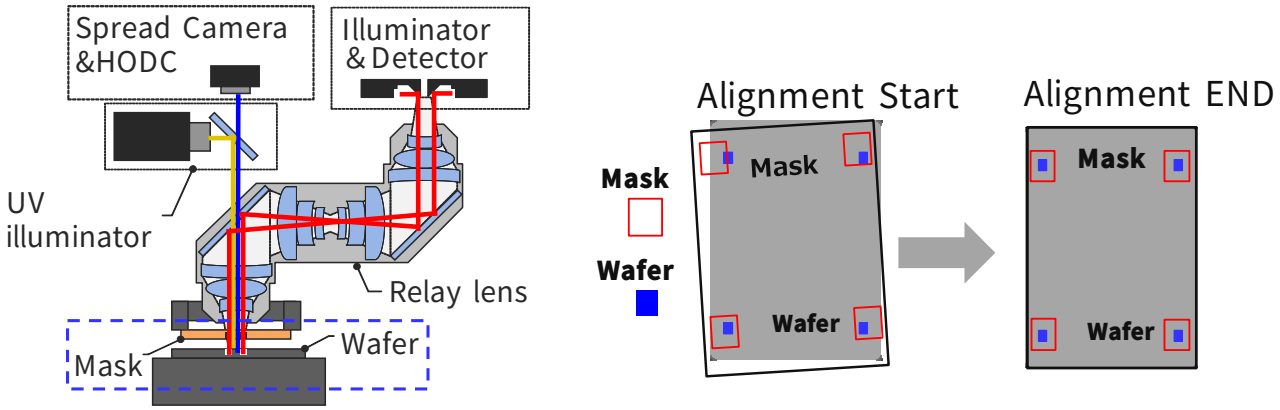

Figure 1. Through The Mask (TTM) alignment system

b. Moiré Alignment Mark Detection

Moiré Alignment marks are used for our TTM alignment. Moiré is generated by mask and wafer gratings. The wafer side grating mark of the moiré is hatched and diffracted in the XY direction. Figure 2a shows a projection view. Figure 2b shows an XZ plane view. Illumination enters from the Y direction orthogonal to the measurement direction. Illumination is transmitted through the mask and diffracted by hatching of the wafer. In the Y direction, illumination is vertically reflected by hatching of the wafer surface. In the X direction, the light is diffracted at a diffraction angle of a wafer pitch $\sin\theta w = \lambda/Pw$. The Illumination diffracted by the wafer goes to the mask and diffracts at an angle determined by the mask pitch $\sin\theta m = \lambda/Pm$. Since the pitch of the wafer and the pitch of the mask are slightly changed, interference light having a small diffraction angle difference ($\lambda/Pw - \lambda/Pm$) is formed. A moiré fringe is generated, and the positional deviation can be measured by measuring the moiré fringe. Illumination is incident from a direction orthogonal to the measurement direction, Illumination is completely dark field.

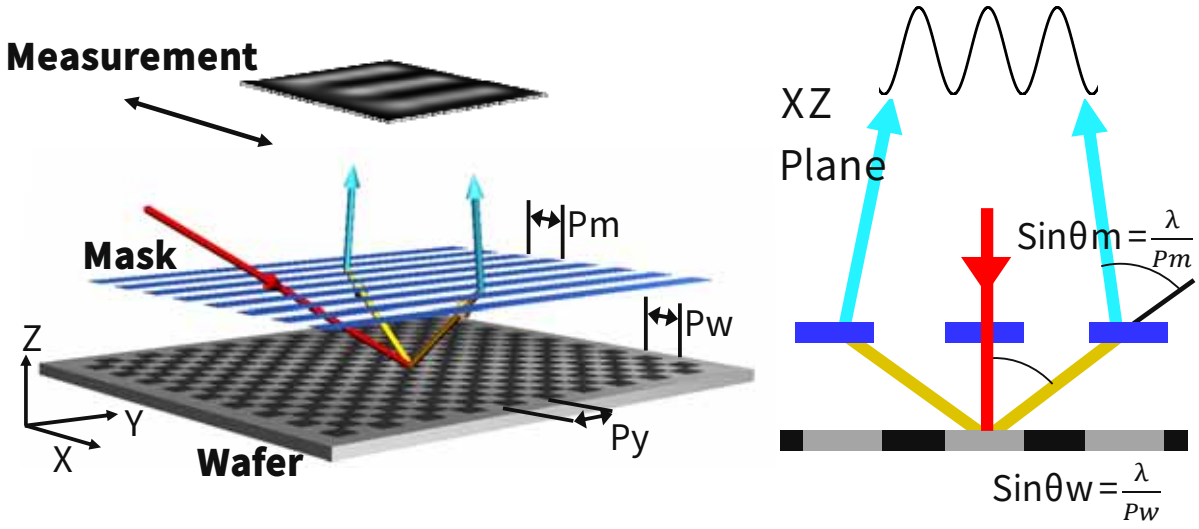

Figure 2. a) Projection view of the moiré alignment mark. b) XZ Plane view of the moiré alignment mark.

c. Illumination for moiré XY direction measurement

The actual marks are shown in Figure 3. Figure 3a shows the mask grating mark. Figure 3b shows the wafer hatching mark. Figure 3c shows a state in which the mask mark and the wafer mark are overlapped, with the XY measurement mark placed close to each other. For XY measurement, we illuminated the entire mark with quadrupole illumination as shown in Figure 4a. Since the illumination orthogonal to the measurement direction is used, the illumination light in the measuring direction causes blooming. The illumination not used for measurement scatters the mark edges and creates blooming light, resulting in measurement errors as shown in Figure 4b. As a result, we improve the illumination method. Y-Dipole illumination is applied to the mark for measuring the X direction, and X-Dipole illumination is applied to the mark for measuring the Y direction as shown in Figure 5a. By changing the illumination condition in each area, we were able to reduce the blooming. We call this "Dual" dipole illumination.

Figure 6 is the results of the Dual dipole illumination. Dual dipole illumination reduces blooming light. The signal of the square area is displayed in a sectional view. Dual dipole illumination reduced the crosstalk of illumination. We have confirmed the noise is reduced to less than 1/5.

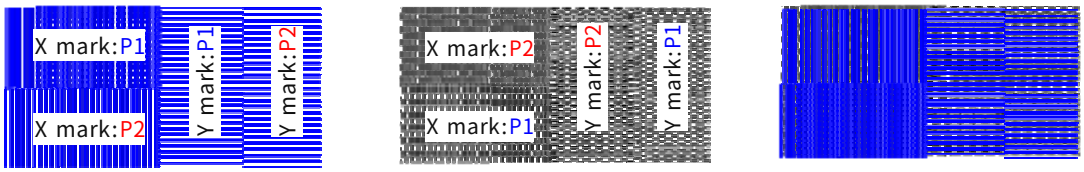

Figure 3. a) TTM mask mark. b) TTM wafer mark. c) Overlapped wafer and mask marks.

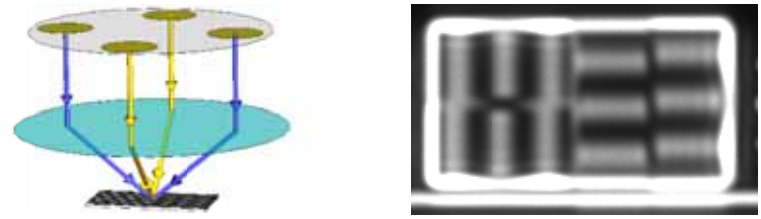

Figure 4. a) Quadrupole illumination. b) Images obtained by quadrupole

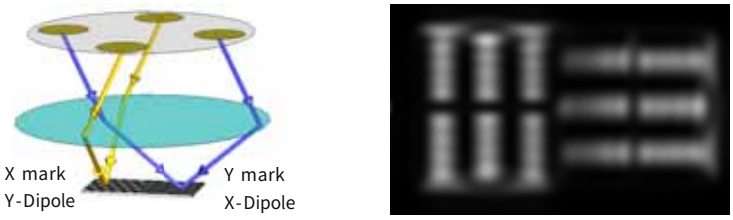

Figure 5. a) Dual Dipole illumination. b) Images obtained by Dual Dipole

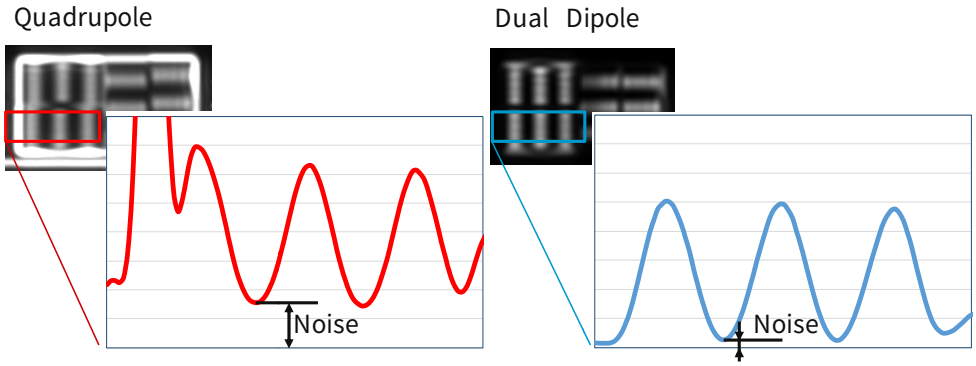

Figure 6. a) Quadrupole Dipole Cross-sectional signal. b) Dual Dipole Cross-sectional signal.

3. Process Robustness Analysis

Robustness enhancement was an important issue for the die by die system because the error of the measured value directly affects the overlay. Therefore, we analyzed in detail how the variation of the film thickness and the mark asymmetry of the creates errors.

a. **Mark asymmetry and film thickness**

The influence of mark asymmetry and film thickness variation on the error is discussed using the model structure of Figure 7a. For simplicity, the alignment mark is defined as a phase object, the thickness and asymmetry of the alignment mark is defined by the ρ(x) equation. ρ(x) is given by C0 and C1 as shown in Figure 7b.

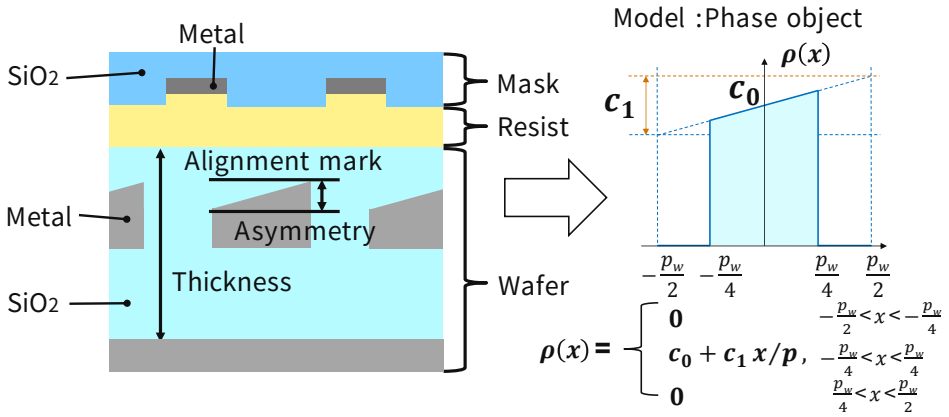

Figure 7. a) Model of the analysis. b) Phase object model of the mark asymmetry.

b. **Measurement error vs. mark asymmetry and film thickness**

Figure 8a shows a phase object and a moiré signal when the film thickness is T and the mark asymmetry is 0. Since there is no mark asymmetry in the mark, the center position of the moiré signal is located at the center position and the measurement error is 0. Figure 8b shows the mark when the film thickness is T and the mark asymmetry is A. The mark asymmetry causes the shift of the peak position of the moiré, resulting in measurement error. Figure 8c shows the mark when the film thickness is T/2 and the mark asymmetry is A, Changes in film thickness with mark asymmetry cause measurement errors. Since the phase actually varies depending on the wavelength, the effect was examined for each wavelength.

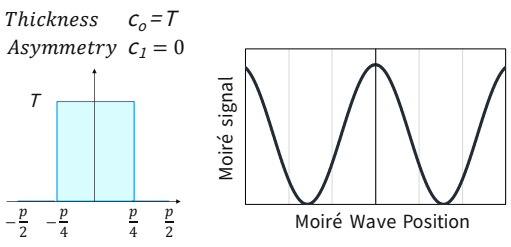

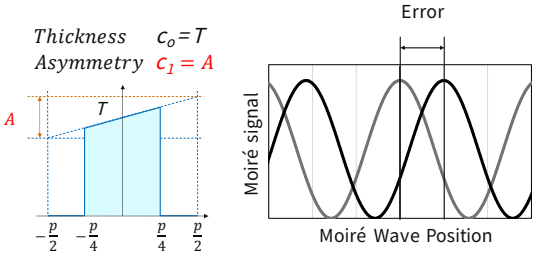

Figure 8. a) Film thickness = T, mark asymmetry=0. b) Film thickness =T, mark asymmetry =A

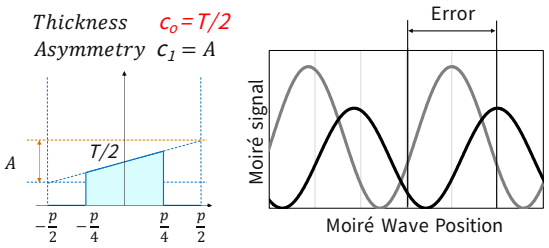

Figure 8. c) Film thickness = T/2. Mark asymmetry = A.

c. **Measurement error vs wavelength**

Figure 9a shows a plot of the measurement error when the mark asymmetry is changed for each wavelength. The horizontal axis is measurement wavelength and the vertical axis is measurement error. The solid line is the original state mark asymmetry is A, and the broken line mark asymmetry is 3A. Since the phase changes according to the wavelength, the measurement error due to asymmetry tended to change from a positive to negative value. When the mark asymmetry changes, the measurement error changes in proportion to the original value. Figure 9b shows a plot of the measurement error when the thickness with asymmetry is changed for each wavelength. The horizontal axis is measurement wavelength and the vertical axis is measurement error. The solid line is the original state film thickness =T' and the broken line is film thickness=T'+ Δ T. Every wavelength has an error in the same direction. The effects of mark asymmetry and film thickness change have been confirmed.

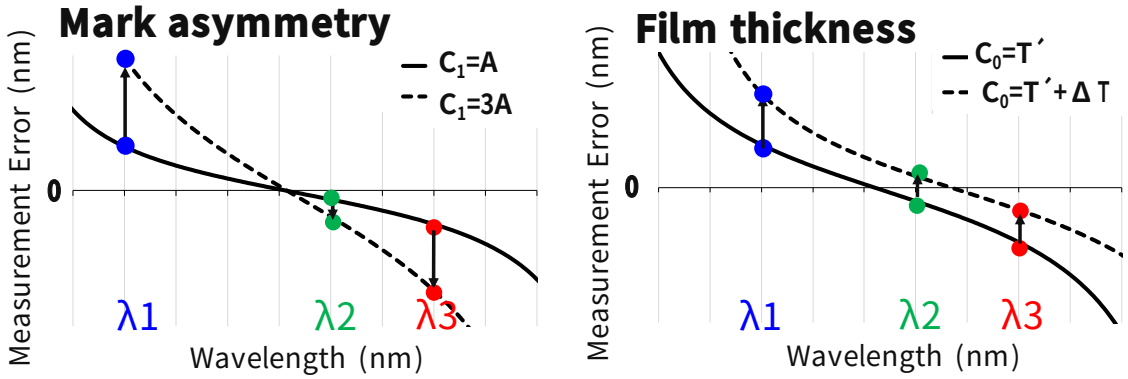

Figure 9. Measurement error vs wavelength. a) Mark asymmetry. b) Film thickness.

3. Experimental Results of Test Wafer

a. Measurement error by 3 wavelengths

In order to confirm the measurement error caused by asymmetry and thickness change, measurements were made by three wavelengths on the same wafer. Three wavelengths were measured at one point per shot. The measurements were compared to adjacent overlay marks. The measurement error between wavelengths was analyzed, and the cause of the measurement error was estimated. By optimizing the wavelength using the result, the optimization to minimize the measurement error was carried out, and the improvement of the measurement robustness was demonstrated.

Figure 10 shows intra wafer measurement errors vector due to three wavelengths. The absolute measurement errors are large at λ1 and λ3 and small at λ2. The distribution of measurement error can be confirmed in the radial direction of the wafer for each wavelength. A graph of alignment mark position and measurement error is shown in Figure 11. Figure11a shows the alignment mark position and the measurement error(X). Figure11b shows the alignment mark position and the measurement error(Y). In both measurement (x) and measurement (y), the measured value is observed to change; λ1 changes to plus direction, λ2 changes to a minus direction, and λ3 changes to minus direction along the alignment position. As described in Section 2, it is mark asymmetry that causes different sign measurement errors for different wavelengths. Figure 12 shows the measurement error when the asymmetry changes. The error was calculated with respect to the thickness conditions of the test wafer. The change in asymmetry change λ1 changes to the plus direction, λ2 changes to a minus direction, and λ3 changes to a minus direction. The trend of change is consistent with the experiment. It is considered that the asymmetry changes in the radial direction of the wafer. The measurement error can be reduced by performing the measurement at an optimized wavelength where the error generated by the asymmetry becomes zero.

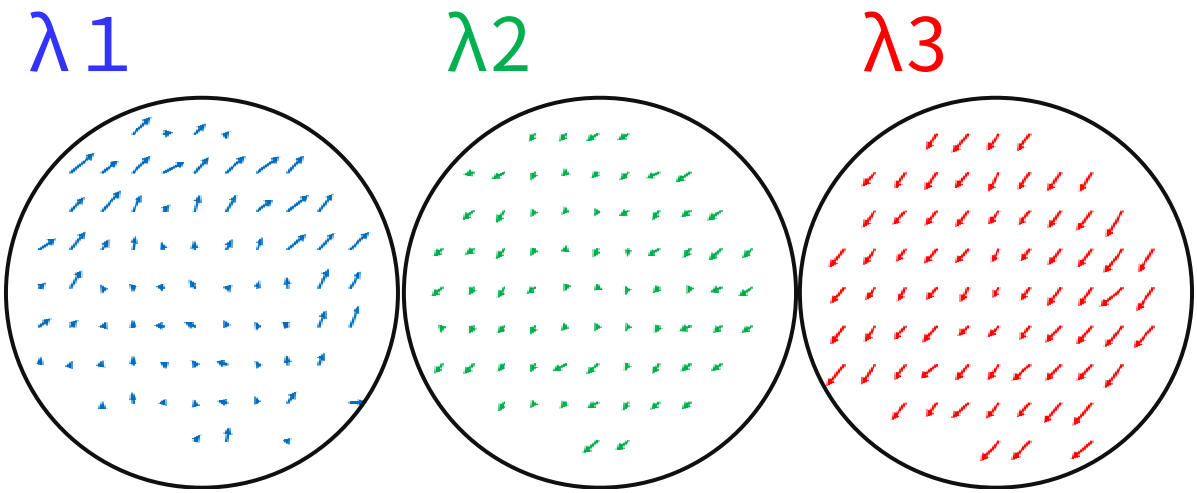

Figure 10. Measurement errors in the wafer plane of λ1, λ2, and λ3.

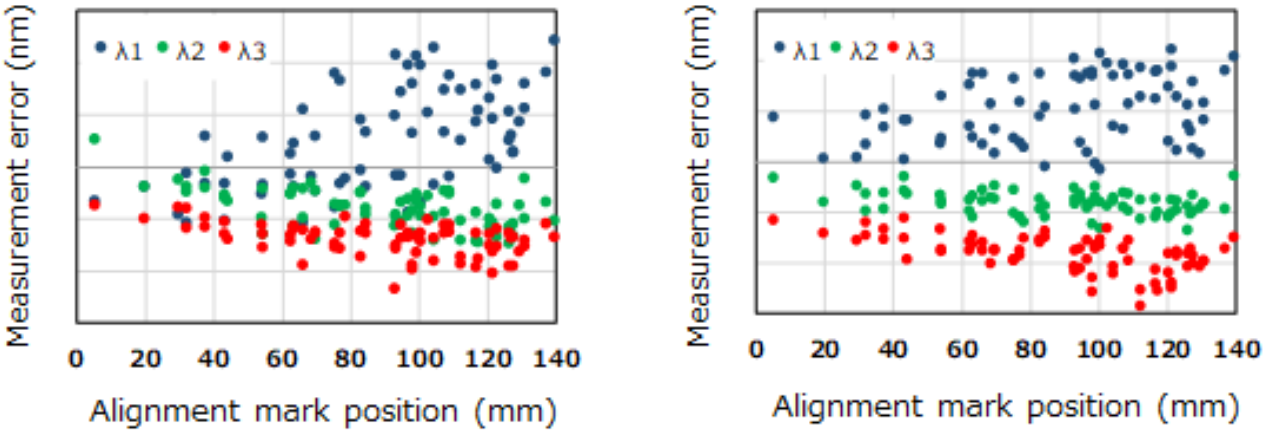

Figure 11. a) Measurement errors (X) vs Alignment mark position (mm). b) Measurement errors (Y) vs Alignment mark position. The measurement error is defined by the TTM-Overlay tool.

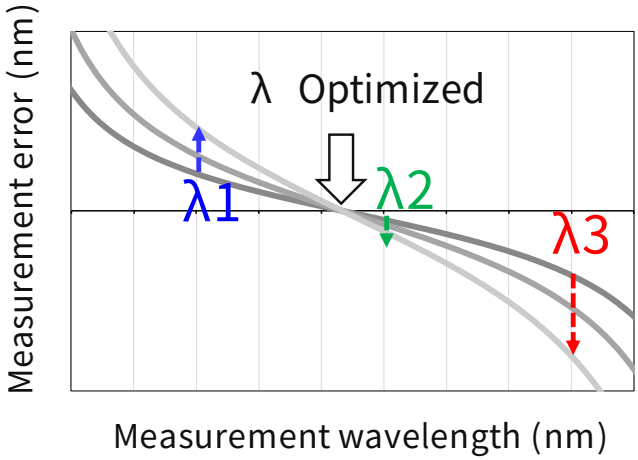

Figure 12. The change in asymmetry error calculated under the conditions of the experiment.

b. Results of optimization of wavelength

FIG. 13 shows results of measurement error (X, Y) vs alignment mark position after wavelength optimization. The vertical scale of the graph is the same as Figure 11. The measurement error tendency depending on the wafer location is reduced. This indicates that the measurement error due to the asymmetry of the mark was reduced by optimization of the wavelength. It is effective to reduce the measurement error by considering whether the measurement error is caused by asymmetry or film thickness.

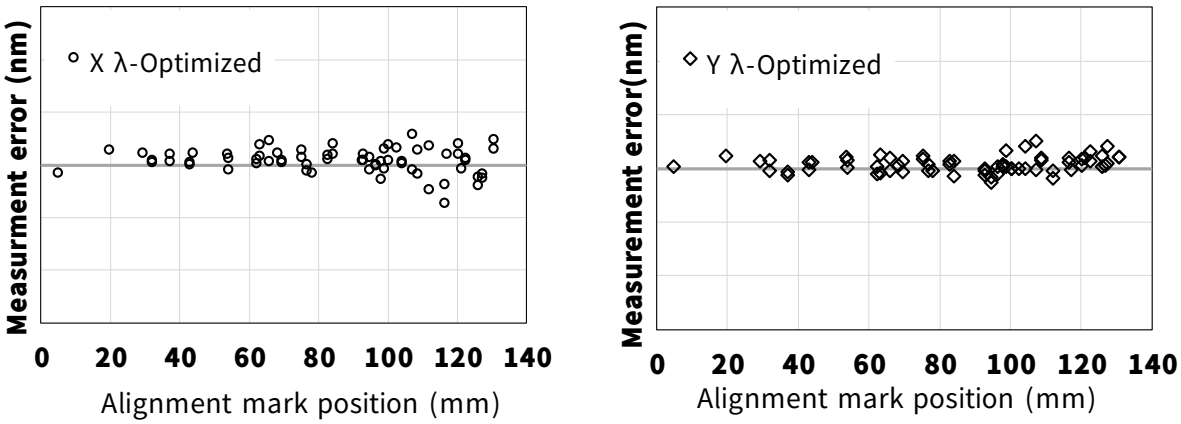

Figure 13. (a) Measurement errors X vs alignment mark position (mm) (b) Measurement errors Y vs alignment mark position (mm).

c. Results of robustness enhancement

The effect of process robustness enhancement by dual dipole and wavelength optimization was confirmed by an experiment on a test wafer lot. The results of comparison between TTM measurement and overlay tool for 24 test wafers are shown in Figure 14. The data was obtained by swinging the offset to check the linearity. One point shows the measurement result of 1 shot. Illumination conditions were improved from quadrupole to dual dipole. The wavelength setting was changed from white to the optimized wavelength.

TTM align measurements improve from 3.6nm to 2.4nm three sigma when compared to the measurements from an Archer overlay tool by applying the dual dipole. Wavelength optimization further reduced the three sigma variation from 2.4 nm to 1.4 nm. As a result, the adoption of dual dipole and wavelength optimization reduced the measurement error of the overlay tool and a TTM variation of 1.4 nm has been achieved.

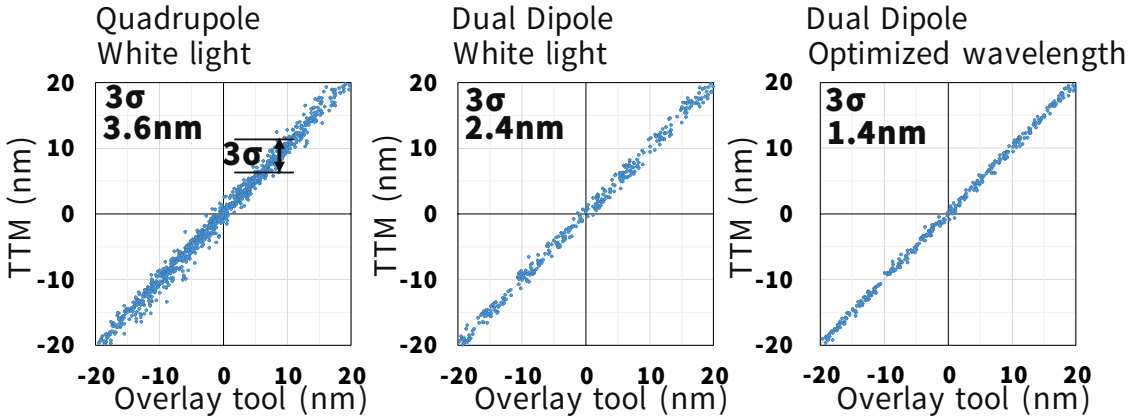

Figure 14. TTM vs Overlay tool measurement error (a) quadrupole white light (b) dual dipole white light (c) dual dipole optimized wavelength

a. XMMO Results

The TTM and HODC systems were applied to test wafers and the results are reported in Figure 15 and 16. Figure 15 depicts Cross Matched Machine Overlay (XMMO) on an existing level patterned with an ASML 1950 ArF immersion tool. A total of 84 fields were measured, including twelve points per field. The results are an average across twenty-five wafers. XMMO of 3.2nm and 2.8nm mean plus three sigma was achieved in x and y, respectively.

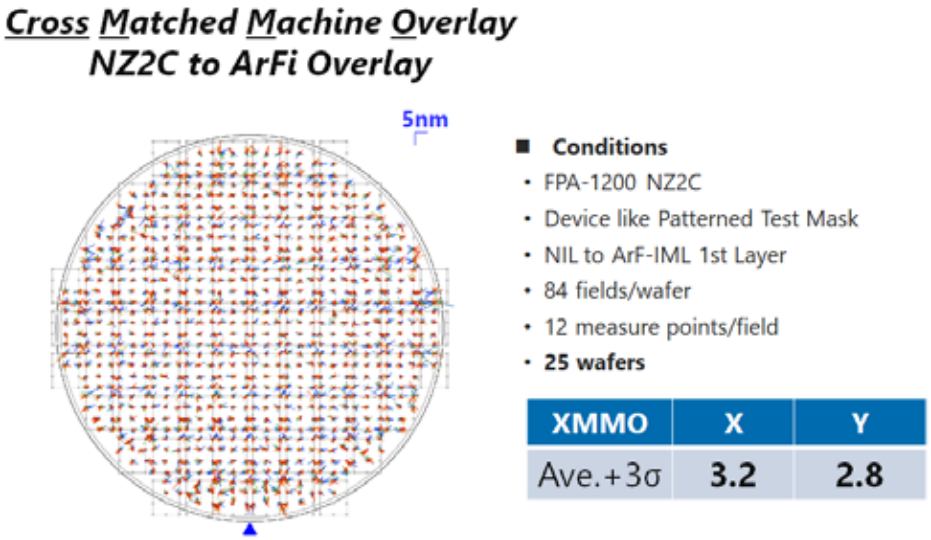

Figure 15. XMMO using an FPA-1200 NZ2C imprint system. XMMO of 3.2nm and 2.8nm mean plus three sigma was achieved in x and y, respectively

Similarly, Figure 16 depicts NIL Mix and Match Overlay (NIL MMO) on an existing level patterned with the FPA-1200 NZ2C tool. A total of 84 fields were measured, including twelve points per field. The results are an average across three wafers. NIL MMO of 2.2nm and 2.4nm mean plus three sigma was achieved in x and y, respectively. Residual distortions were 0.7nm, mean plus three sigma.

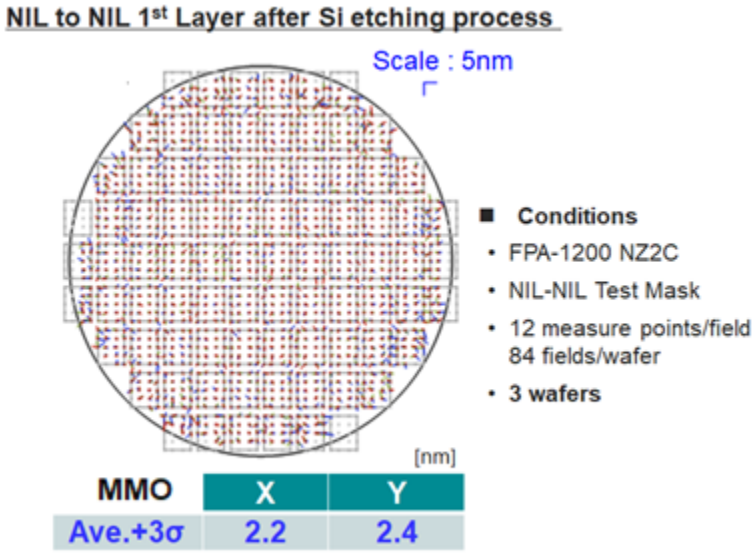

Figure 16. NIL MMO using an FPA-1200 NZ2C imprint system. MMO of 2.2nm and 2.4nm mean plus three sigma was achieved in x and y, respectively

4. Conclusions

Canon developed a through-the-mask moiré alignment system for the FPA-1200NZ2C nanoimprint lithography (NIL) system allowing high-speed measurement of several alignment marks within each imprint field and alignment compensation to be completed during the imprinting sequence. To provide increased process flexibility, overlay accuracy while maintaining high-productivity, we have been developed a new low-noise, high-resolution, high-robustness moiré diffraction alignment system based on spatial phase interferometry. By applying dual dipole illumination and wavelength optimization, measurement errors have been reduced to less than 40%. Mass production level robustness has been achieved. On test wafers, XMMO of 3.2nm and 2.8nm in x and y respectively was demonstrated across a 25 wafer lot. Further improvements to the align system have been realized with a multi-wavelength strategy and machine learning.

References

1. S. Y. Chou, P. R. Kraus, P. J. Renstrom, “Nanoimprint Lithography”, J. Vac. Sci. Technol. B 1996, 14(6), 4129 - 4133.
2. T. K. Widden, D. K. Ferry, M. N. Kozicki, E. Kim, A. Kumar, J. Wilbur, G. M. Whitesides, Nanotechnology, 1996, 7, 447 - 451.
3. M. Colburn, S. Johnson, M. Stewart, S. Damle, T. Bailey, B. Choi, M. Wedlake, T. Michaelson, S. V. Sreenivasan, J. Ekerdt, and C. G. Willson, Proc. SPIE, Emerging Lithographic Technologies III, 379 (1999).
4. M. Colburn, T. Bailey, B. J. Choi, J. G. Ekerdt, S. V. Sreenivasan, Solid State Technology, 67, June 2001.

5. T. C. Bailey, D. J. Resnick, D. Mancini, K. J. Nordquist, W. J. Dauksher, E. Ainley, A. Talin, K. Gehoski, J. H. Baker, B. J. Choi, S. Johnson, M. Colburn, S. V. Sreenivasan, J. G. Ekerdt, and C. G. Willson, Microelectronic Engineering 61-62 (2002) 461-467.
6. S.V. Sreenivasan, P. Schumaker, B. Mokaberi-Nezhad, J. Choi, J. Perez, V. Truskett, F. Xu, X, Lu, presented at the SPIE Advanced Lithography Symposium, Conference 7271, 2009.
7. K. Selenidis, J. Maltabes, I. McMackin, J. Perez, W. Martin, D. J. Resnick, S.V. Sreenivasan, Proc. SPIE Vol. 6730, 67300F-1, 2007.
8. I. McMackin, J. Choi, P. Schumaker, V. Nguyen, F. Xu, E. Thompson, D. Babbs, S. V. Sreenivasan, M. Watts, and N. Schumaker, Proc. SPIE **5374**, 222 (2004).
9. K. S. Selinidis, C. B. Brooks, G. F. Doyle, L. Brown, C. Jones, J. Imhof, D. L. LaBrake, D. J. Resnick, S. V. Sreenivasan, Proc. SPIE 7970 (2011).
10. Y. Takabayashi, T. Iwanaga, M. Hiura, H. Morohoshi, T. Hayashi, and T. Komaki, Proc. SPIE 10958 (2019) 109580B
11. Kohei Imoto et al., Proc. SPIE. 10451, Photomask Technology, 104511B (2017).
12. Yukio Takabayashi et al., Proc. SPIE. 10144, Emerging Patterning Technologies, 1014405 (2017).